Alexandria Engineering Journal (2022) 61, 709–718

HOSTED BY

ELSEVIER

Alexandria University

Alexandria Engineering Journal

www.elsevier.com/locate/aej
www.sciencedirect.com

Modified phase correlation algorithm for image registration based on pyramid

Yang Li [a,b,*], Jianli Wang [a], Kainan Yao [a]

[a] *Changchun Institute of Optics, Fine Mechanics and Physics, Chinese Academy of Sciences, Changchun 130033, China*
[b] *University of Chinese Academy of Sciences, Beijing 100049, China*

Received 22 February 2021; revised 21 April 2021; accepted 3 May 2021
Available online 5 June 2021

KEYWORDS

Panoramic target detection system;
Image registration;
Pyramid phase correlation algorithm;
Deep learning

Abstract Image registration is an important process for applications in various fields, such as remote sensing and medical imaging; thus, its accuracy significantly affects the efficacy as well as efficiency of those applications. Phase correlation algorithm (PCA) and normalized cross correlation-pyramid (NCCP) algorithm are the state-of-the-art frequency domain and spatial domain methods for image registration, respectively. However, these algorithms have some limitations. In particular, the registration speed of PCA needs to be improved, while the NCCP algorithm leads to errors if the image to be registered is partially occluded. Thus, to overcome these limitations, we propose a pyramid PCA that combines both algorithms. To verify the performance of our proposed algorithm, its results are compared with those obtained using the traditional PCA and NCCP algorithm. Our simulation results for partially occluded images indicate that the proposed algorithm outperforms the NCCP algorithm in terms of accuracy; in addition, it outperforms PCA in terms of speed. Furthermore, to test the feasibility of the proposed algorithm for real-time applications, a panoramic target detection system was set up, and the results obtained using the system proved that our method for image registration was both feasible and effective.

1. Introduction

Image registration is the process of overlaying two or more images of the same scene captured at different times, from different viewpoints, and/or by different sensors [1–4]. Image registration is a crucial process in many image processing applications that need to integrate multiple images for analysis; these applications include scene change detection, image mosaics, image fusion, and medical imaging [5–9]. In addition, accurate image matching via image registration is important for subsequent processing of collected remote sensing data [10,11].

The methods adopted for image registration can be broadly classified into spatial domain [12–16] and frequency domain methods [17–22]. The direct method is an important way of spatial domain registration, it involve pixel-by-pixel comparison, wherein the pixel intensities of one image are compared

* Corresponding author at: Changchun Institute of Optics, Fine Mechanics and Physics, Chinese Academy of Sciences, Changchun 130033, China.
E-mail address: liyang940517@126.com (Y. Li).

Peer review under responsibility of Faculty of Engineering, Alexandria University.

https://doi.org/10.1016/j.aej.2021.05.004
1110-0168

to the other image. In practice, a direct method uses all pixel intensities of an image to register two images [23]. In particular, this direct approach makes use of a cost function or the sum of the absolute differences (SAD) between overlapping pixels to combine images [24]. Several traditional direct image registration algorithms are based on gray information; examples of such traditional registration algorithms are SAD, sum of squared differences (SSD), and normalized cross correlation (NCC) algorithms. The primary advantage of the direct methods is that they optimally use image alignment information; thus, these methods are useful for registration of images with large overlapping regions, involving only small translations and rotations. However, a direct registration method has the following limitations: (1) It is sensitive to grayscale changes in the image, especially nonlinear illumination changes, which significantly reduce the performance of such an algorithm. (2) Because the gray information of the entire image is considered in such a method, the calculations required are extensive, and consequently, the registration speed is slow. (3) Only grayscale features of an image are used for registration whereas the contribution of other features of the image is neglected. Consequently, grayscale-based image registration is sensitive to noise. (4) Grayscale-based methods have poor stability, i.e., they easily fall into local extremes, leading to mismatches. The NCC image matching algorithm based on gray correlation can provide accurate results, but it will take a lot of time to perform a lot of calculations, Fouda and Ragab [41] proposed a pyramid-based NCCP to reduce time. We are inspired by this to use a pyramid strategy to reduce the computational complexity of the algorithm.

In contrast, literature on frequency domain based cross-correlation, and phase-only correlation is reported in [25–29]. Recently Xu and Varshney [30] have specified the application of a subspace-based frequency estimation approach for the Fourier based image registration problem. They have used multiple signal classifier algorithm for more robust and accurate results resulting into moderate increase in computational complexity. Correlation Technique was used to refine the user-defined landmark positions to register tomographic brain [31] and abdominal images [32]. Collignon et al. has suggested the use of the Entropy Correlation Coefficient (ECC), for image registration using normalized mutual information [33,34]. Sanjay-Gopal et al. [35] have compared mutual information and the correlation coefficient for registration of intra-subject mammograms. Samritjiarapon and Chitsobhuk [36]. have used Fourier based technique along with best-first search algorithm to find the translation between two input images. The Fourier-based technique is used to estimate the candidate translations to decrease searching space while best-first search algorithm is used to further search for the correct translation. This technique can estimate large translations, scalings, and rotations in images by an extension of phase correlation technique. They focus on increased accuracy of this technique to detect large translations compared to the other techniques in frequency domain. In the above cases, the direct methods and phase correlation algorithm (PCA), are too slow for real-time applications and prone to errors when the image to be registered is partially occluded. Thus, there is a need for a registration algorithm that not only achieves registration and fast matching, but also is strongly robust to partially occluded images.

In the panoramic target detection system, the image registration algorithm is often required to have a faster speed, and the image registration algorithm is strongly robust to the case of the target is partially lost or occluded, so we propose a pyramid PCA algorithm that combines the PCA and NCCP algorithms. The pyramid PCA algorithm has the advantages of pyramid PCA and NCCP algorithms at the same time, which can meet actual needs.

The remainder of the paper is organized as follows. Section 2 describes the pyramid PCA; in addition, the speed of the algorithm is verified by analyzing its computational complexity. In Section 3, we present the numerical simulation results, which show that the proposed algorithm is not only better than the state-of-the-art normalized cross correlation-pyramid algorithm for image registration in the case of partially occluded targets, but also is faster than PCA. Section 4 discusses our panoramic target detection system using which the effectiveness of our algorithm is verified for real-time applications. Finally, Section 5 concludes the paper and presents directions for future research.

2. Theory and proposed image registration algorithm

Given a source image S and template image T of size $p \times q$ and $m \times n$, respectively, as shown in Fig. 1, our objective is to accurately and efficiently calculate the best match position for template T in the source image S. First, the proposed pyramid PCA is discussed below. Next, we theoretically analyze the superiority of our proposed algorithm over traditional algorithms.

2.1. Pca

In terms of signal processing of images, the correlation between two image signals can be achieved by the convolution of the two signals, which, in turn, can be used to compare the similarities between the images. In addition, when the image is analyzed in the frequency domain, its Fourier spectrum con-

(a) (b)

Fig. 1 Image of peppers: (a) Source image of size 800×800 containing the template pattern (b) Template image of size 300×300.

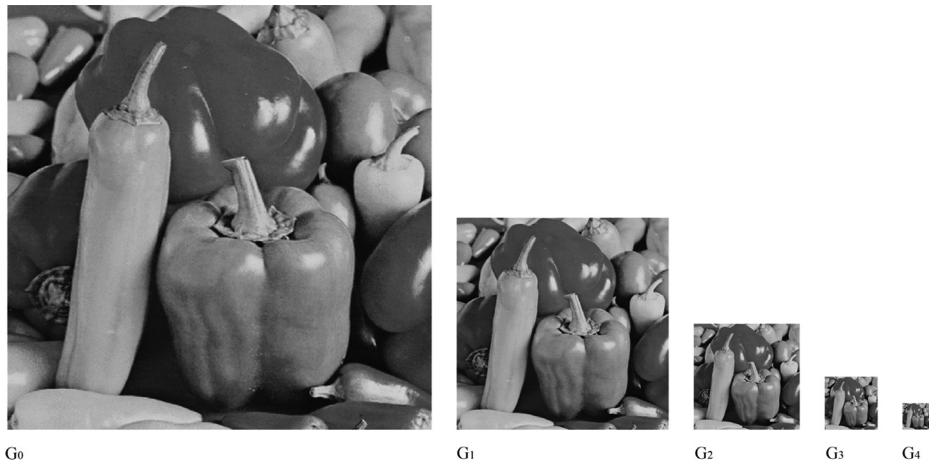

Fig. 2 Gaussian pyramid.

tains both modulo and phase information. The modulo represents the gray level information of the image, while the phase represents its texture and structure information. For an image $I(x,y)$, its complex spectrum $I_f(u,v)$ includes both amplitude and phase information; in turn, the phase information contains the position information of the original image $I(x,y)$. Therefore, by calculating the correlation of the phases between two images, the difference between the images can be obtained, thereby enabling their registration. Thus, using the phase spectrum matching method, the proposed PCA can solve the image registration problem through simple shifting. The PCA is a popular Fourier domain method used to register two images. It computes a phase difference map that (ideally) contains a single peak. The location of the peak is proportional to the relative translation $[dx, dy]$ between the two images [37]. The PCA is equivalent to correlation in the spatial domain, but the calculation is orders of magnitude faster in the Fourier domain. The mathematical details are as follows:

Consider two identical images i1 and i2, with i2 shifted by an amount $[\Delta x, \Delta y]$ relative to i1:

$$i2(x,y) = i1(x - \Delta x, y - \Delta y) \tag{1}$$

These images obey the following periodic boundary conditions:

$$i1(M + x, N + y) = i1(x,y) \tag{2}$$

where the image size is $M \times N$ pixels. Denote Fourier transforms of i1 and i2 as I1 and I2. From the Fourier shift theorem, I1 and I2 differ only by a linear phase term $j(\omega_x \Delta x + \omega_y \Delta y)$. In particular,

$$I2(\omega_x, \omega_y) = I1(\omega_x, \omega_y) e^{-j(\omega_x \Delta x + \omega_y \Delta y)} \tag{3}$$

where $I2(\omega_x, \omega_y)$ and $I1(\omega_x, \omega_y)$ are the corresponding Fourier transforms of i1(M + x,N + y) and i1(x,y). The normalized cross-power spectrum of the images, C12, is defined as follows:

$$C12(\omega_x, \omega_y) = \frac{I2^*_{\cdot} conj(I1)}{|I2^*_{\cdot} conj(I1)|} = e^{-j(\omega_x \Delta x + \omega_y \Delta y)} \tag{4}$$

The operator * is the Schur product (also known as the Hadamard element-by-element matrix product) and conj is the complex conjugate operator.

Eq. (5) is an inverse Fourier transform of C12. The result of the transformation is a two-dimensional Dirac delta function $\delta(x - \Delta x, y - \Delta y)$ with a peak location corresponding to the displacement $[\Delta x, \Delta y]$ between the two images. Finally, the coordinates corresponding to the peak point of the function can be obtained, which, in turn, can be used to calculate the required registration position.

$$\mathscr{F}^{-1}(e^{-j(\omega_x \Delta x + \omega_y \Delta y)}) = \delta(x - \Delta x, y - \Delta y) \tag{5}$$

2.2. Modified PCA

The modified PCA combines the traditional PCA with the pyramidal approach. It is primarily based on pyramid scaling. The workflow of the algorithm is described below.

(1) Image pyramid principle

The concept of compressing and storing images as a pyramid is an important one in the field of template matching algorithms. The image pyramid technique does not perform the process of template matching itself; however, it enhances the speed of template matching algorithms [38,39]. An image pyramid consists of a sequence of copies of an original image in which both sample density and resolution are decreased in regular steps. The reduced resolution levels of the pyramid are obtained through an efficient iterative algorithm. For example, a pixel in an upper layer of an image pyramid summarizes four pixels in the next layer [40]. If multiple pyramid scaling operations are performed, an exponential increase can be realized in image processing speeds. A five-tap filter was used to generate the image pyramid shown in Fig. 2. The bottom or zero level of the pyramid, G_0, is the original image. This is lowpass-filtered and subsampled by a factor of two to obtain the next pyramid level, G_1. G_1 is then filtered in the same manner and subsampled to obtain G_2. Further repetitions of the filter/subsample steps generate the remaining pyramid levels. In particular, the levels of the pyramid are obtained iteratively as follows. For $0 < l < N$:

$$G_l(i,j) = \sum\nolimits_m \sum\nolimits_n w(m,n) G_{l-1}(2i + m, 2j + n) \tag{6}$$

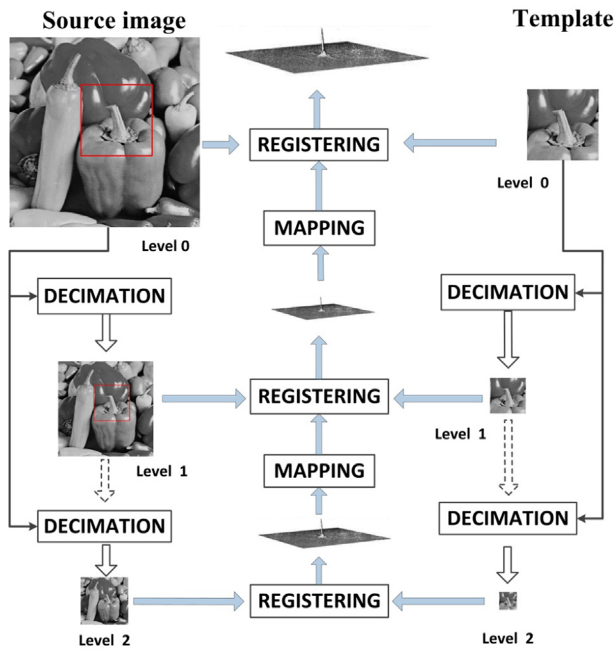

Fig. 3 Pyramid registration scheme.

Original image, G_0 is repeatedly filtered and subsampled to generate the sequence of reduced resolution images G_1, G_2, and so on. These reduced resolution images are a set of lowpass-filtered copies of the original image in which the bandwidth decreases in one-octave steps.

However, this process can be conveniently represented as a standard REDUCE operation, and be written as follows:

$$G_l = REDUCE[G_{l-1}] \tag{7}$$

The weighting function $w(m, n)$ is referred to as the "generating kernel."

(2) Registering images in each level

Fig. 3 shows the workflow for pyramid registration; here, a pyramid with three levels of source and template images is presented. The image registration was performed as follows. First, we acquired the pyramid structure, sub-templates, and sub-sources, using both template and source images. Level 0 indicated the original image, while Level 2 represents the smallest subsampled image. Second, we performed the registration process by mapping the sub-origin from the top level in the pyramid-shaped structure to the bottom level, which is the same as original PCA. The steps to achieve this are as follows:

(1) The sub-templates and sub-sources of Level 2 are registered using the PCA to obtain the registration position for Level 2.

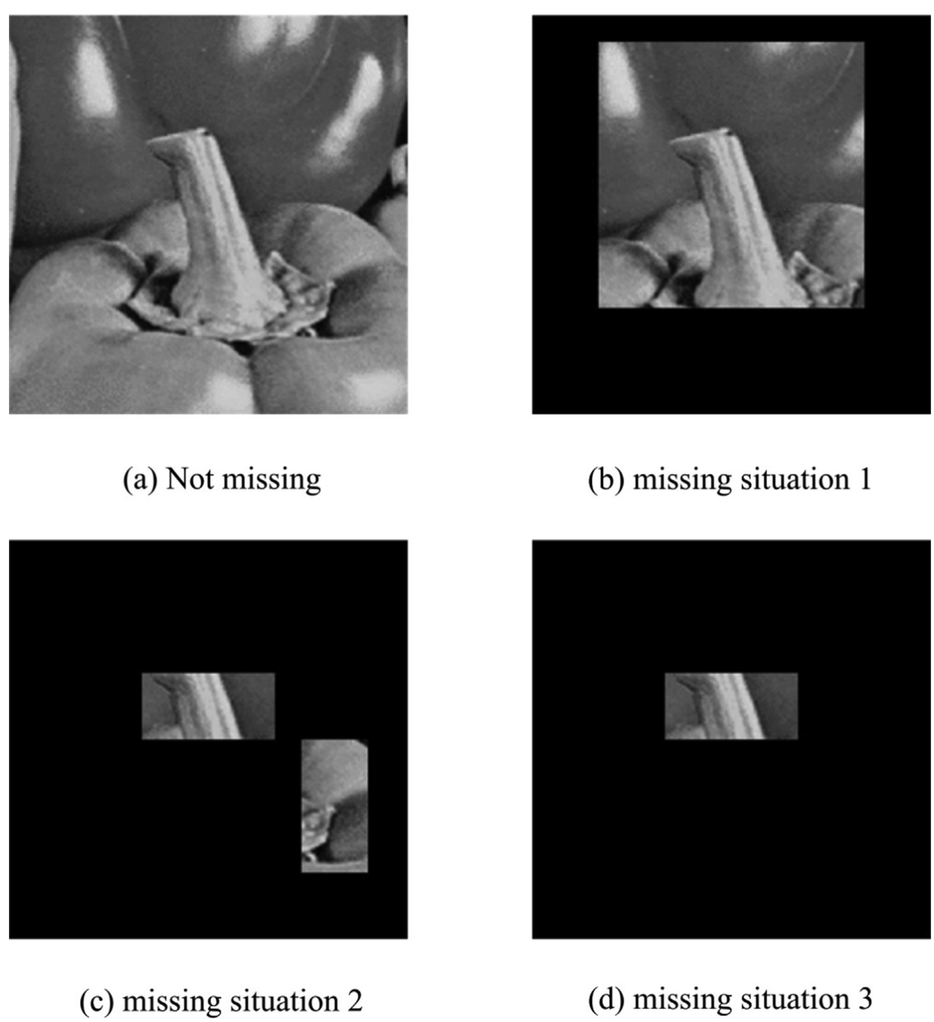

Fig. 4 Peppers image after an ideal translation of Δ and test images with partial occlusions in the target.

(2) The registration position of Level 2 is mapped to Level 1 by acquiring the local area (red rectangular box area) in Level 1 based on the calculated position in the previous step.

(3) The red rectangular box area in Level 1 is registered with the sub-template in Level 1 using PCA to obtain the required registration position.

(4) Steps 2 and 3 are repeated to obtain the final registration position at Level 0.

2.3. Algorithm complexity analysis

The time complexity of the pyramid-based normalization correlation algorithm [41] is $O(n^2)$. The PCA uses fast Fourier transform (FFT); an FFT rapidly computes the previously described transformations by factorizing the discrete Fourier transform (DFT) matrix into a product of sparse (mostly zero) factors. Consequently, the time complexity of the traditional PCA [17] is $O(n\log n)$, where n represents the amount of data of the registered image in the pyramid-based normalization correlation algorithm or the traditional PCA. Accordingly, because a three-level pyramid is used in our proposed algorithm, its time complexity is $\left(\frac{1}{4}\right)^2 O(n\log n)$. Thus, if a k-layer pyramid is used, the complexity of the algorithm is $\left(\frac{1}{4}\right)^{k-1} O(n\log n)$. Considering this, theoretically, an increase in the number of pyramid layers will lead to an exponential increase in image processing speeds; naturally, this indicates that our algorithm will be the fastest compared with other traditional algorithms owing to the use of a pyramid structure.

3. Numerical simulations

For practical real-time applications, the speed required for an image registration algorithm is often higher than in the case of offline processing. In addition, the algorithm needs to be strongly robust to cases wherein the target is partially lost or occluded. In order to verify the performance of the pyramid PCA proposed in our study, it is compared with the pyramid-based normalization correlation algorithm and traditional PCA.

3.1. Comparison between proposed algorithm and pyramid-based normalization correlation algorithm

For our experiment, we used an 800×800 image of Peppers as the source image, which is shown in Fig. 1(a), while we used a 300×300 partial image of Peppers as the template image, which is shown in Fig. 1(b); the ideal offset of the template image is $\Delta = (200, 300)$. For registration positioning, because the target might be partially missing or occluded after relative motion, the registration algorithm is still required to have strong robustness to achieve high-precision positioning of the target. Presuppose the arbitrariness of the template image, for which the ideal template image is shown in Fig. 4(a); if any part of the

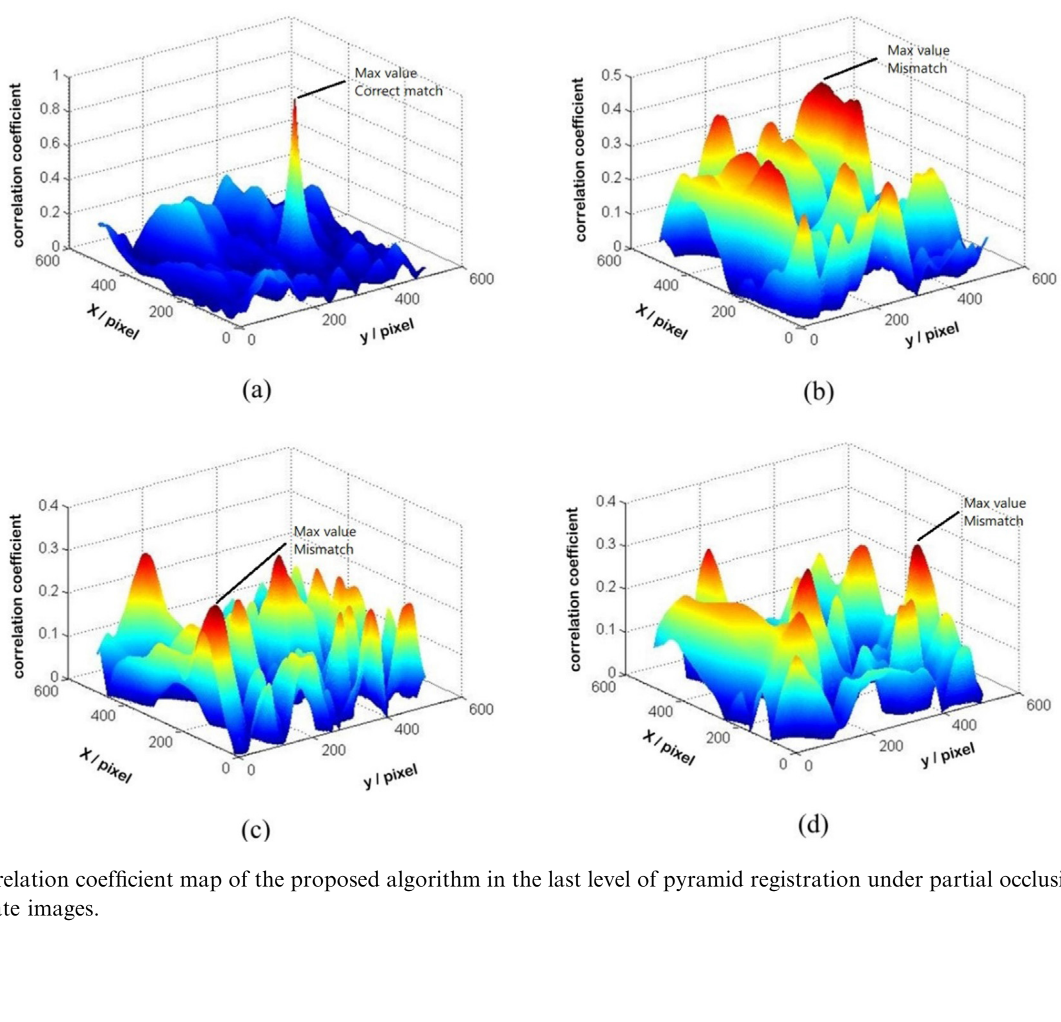

Fig. 5 Correlation coefficient map of the proposed algorithm in the last level of pyramid registration under partial occlusion conditions in the template images.

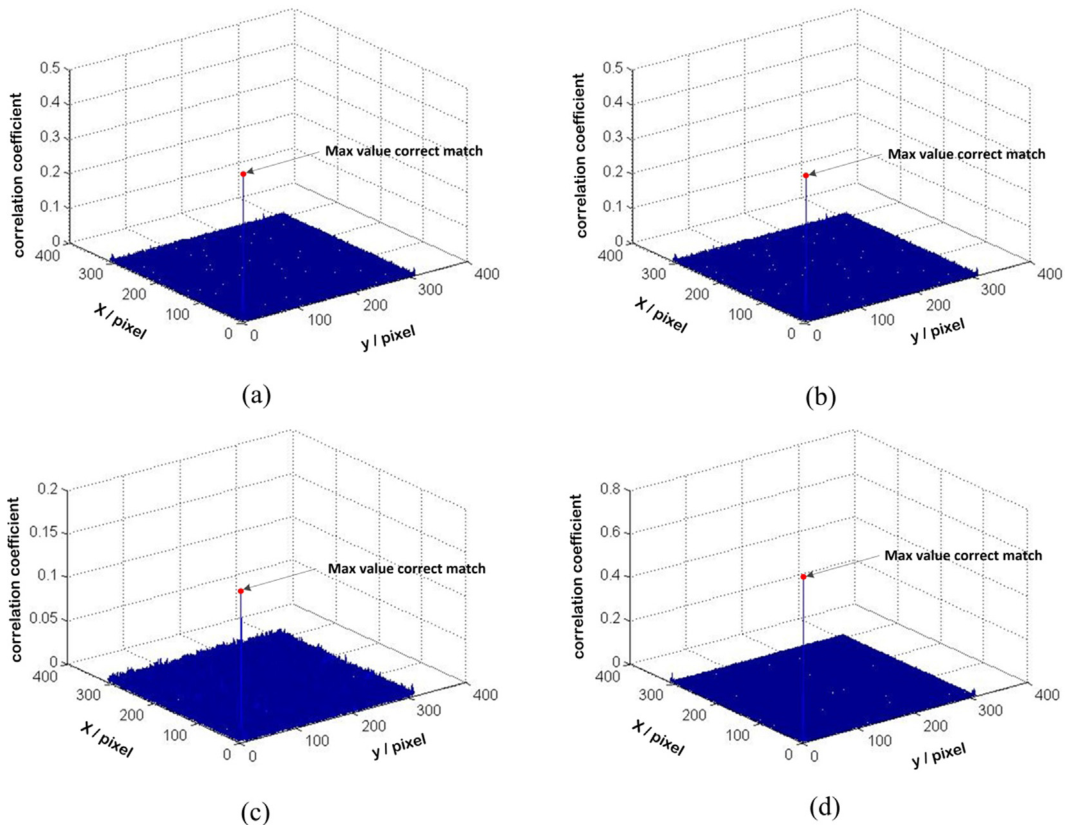

Fig. 6 Correlation coefficient map of the pyramid-based normalization correlation algorithm under partial occlusion conditions in the template images.

template image is missing or occluded, as shown in Fig. 4(b)-(d), the correlation coefficient maps and positioning results obtained using our proposed algorithm and the pyramid-based normalization correlation algorithm are obtained as those shown in Figs. 5 and 6, and listed in Table 1, respectively.

It can be seen from Fig. 5 that the partial absence of the positioning target leads to multiple peaks in the cross-correlation spectrum, and thus, the maximum value obtained by the search cross-correlation spectrum might not be able to locate the correct peak, thereby causing an error in offset detection. Based on the results listed in Table 1, it is clear that the pyramid-based normalization correlation algorithm could not correctly detect the amount of translation required for image registration when the target was partially missing. In contrast, our proposed algorithm achieved template positioning even when the target was partially missing. Furthermore, it can be seen from Fig. 6 that the peak position of the inverse Fourier transform of the phase correlation spectrum is always constant when the positioning target portion is missing.

Table 1 Registration results of the proposed algorithm and that pyramid-based normalization correlation algorithm under partial occlusion conditions in the template images.

Image	Pyramid-based Normalization Correlation Algorithm	Proposed Algorithm
Fig. 4(a)	(200, 300)	(200, 300)
Fig. 4(b)	(446, 395)	(200, 300)
Fig. 4(c)	(123, 33)	(200, 300)
Fig. 4(d)	(355, 453)	(200, 300)

3.2. Comparison between proposed algorithm and the traditional PCA

To test the speed of the two registration algorithms, we used images of different sizes for testing. The size of these images to be registered ranged from 400×400 up to 1600×1600 in steps of 200, with the corresponding template image sizes ranging from 100×100 up to 400×400 in steps of 50, respectively. The registration algorithms that are compared for speed include PCA and our proposed pyramid PCA. Fig. 7 shows the simulation results for the time taken to achieve image registration for different image sizes using the different registration algorithms; in particular, the abscissa represents the side length of the square image, while the ordinate represents the time taken to achieve image registration. From the results, it can be inferred that our pyramid PCA takes lesser time than PCA to achieve image registration. In this registration experiment, we used a three-level pyramid; however, as previously mentioned, the larger the number of pyramid levels, the shorter the time taken for registration. This confirms that the use of image pyramids can effectively reduce the time taken for registration.

4. Experimental setup and results

Image registration is a very important part of image preprocessing in the circle-scan target detection system. in order to detect and identify the target accurately, the images need to be registered fastly and accurately. In order to verify that registration speed of the proposed algorithm is suitable for real-time applications, while ensuring high registration accuracy, we developed a panoramic target detection system. This system rotates every 4 s, capturing one picture every 5° of rotation; therefore, 72 images are captured in every rotation. Because of the vibration of the turntable during rotation, the image has a shift of about 20 pixels in the vertical direction. Furthermore, the field of view of the lens (7.36°) is larger than the image acquisition interval (5°); thus, overlaps and shifts also occur in the horizontal direction. The objective of this

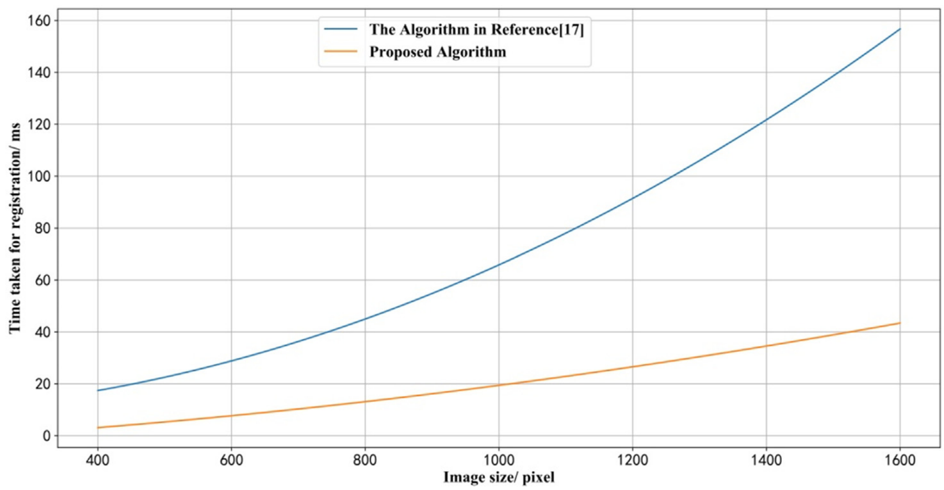

Fig. 7 Time taken by various algorithms to achieve image registration for different image sizes.

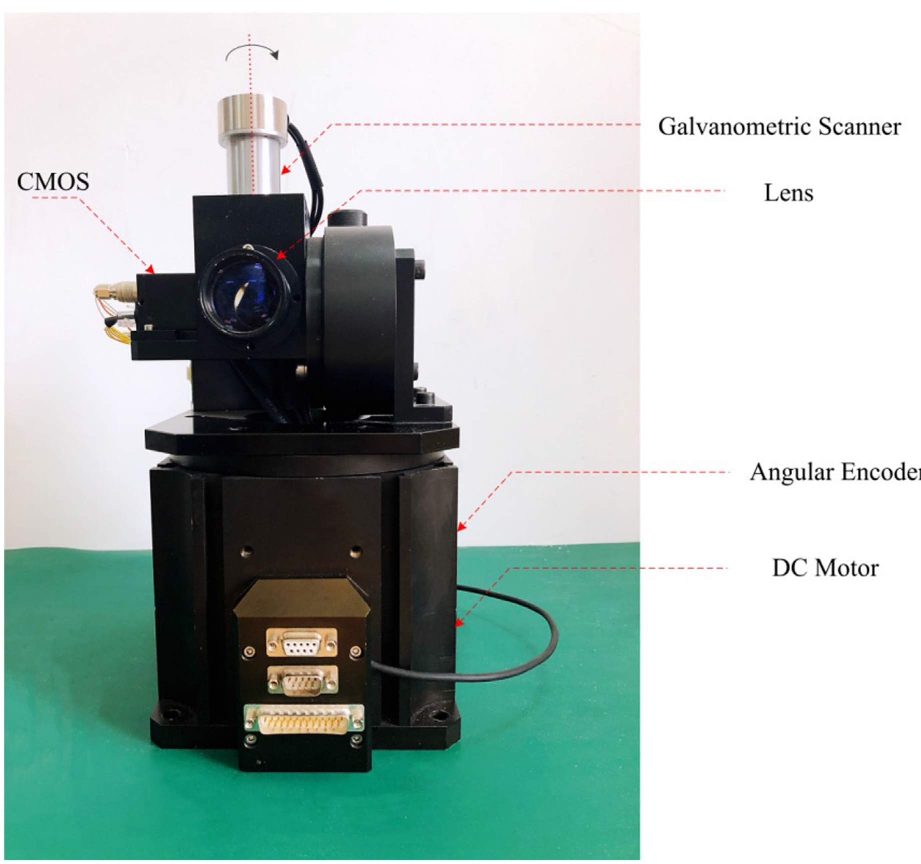

Fig. 8 Physical image of the panoramic target detection system.

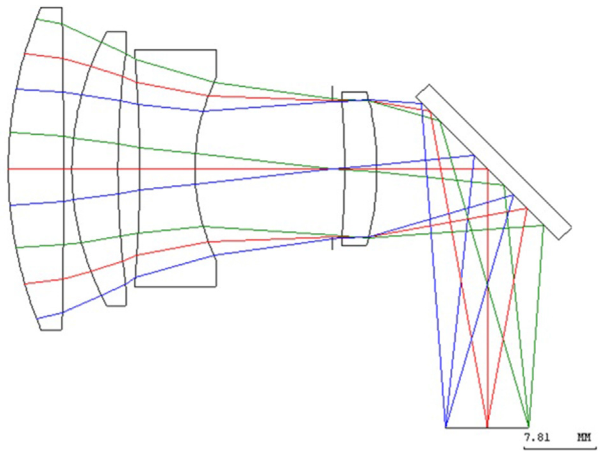

Fig. 9 Optical path diagram of the panoramic target detection system.

experiment is to register and stitch the captured images in real time to form a 360° panorama. This is because image registration with horizontal and vertical shifts is the focus of our research. Finally, we use a deep learning algorithm to identify the category and location of targets in the panorama. This system can play an important role in early warning security applications. Fig. 8 shows the physical image of the developed panoramic target detection system, which consists of a DC motor, angular encoder, galvanometric scanner, and camera.

The CMOS in the panoramic target detection system uses a Mindvision MV-GE200GM-T model with a resolution of 1600×1200 and frame rate of 60 fps; the focal length of the lens is 70 mm, clear aperture is 25 mm, target size is 1/1.8 in., and diagonal size is 9 mm. The maximum scanning angle of the galvanometric scanner is $\pm 15^{\circ}$ and its resolution is 12 uRad. Considering the requirements for the lens (shown in Fig. 9), a four-piece lens was used in the system. The distance between the first and last lens is 40 mm; furthermore, the first lens has a clear aperture of 32.6 mm, while the last one has a clear aperture of 15 mm with a working distance of 40 mm. A galvanometric scanner is installed in this working distance.

Fig. 10 shows the 12 images captured using our panoramic device. These images are spliced and divided into upper and lower layers with 6 images per layer. These images were obtained after we removed some of the overlapping horizontal pixels; however, it can still be observed that the images are offset both horizontally and vertically. If these images are directly placed together to form a panoramic image, not only will they appear visually contradictory, but also subsequent recognition algorithm on using this panoramic image will lead to invalid

Fig. 10 Twelve images captured by the panoramic target detection system for registration.

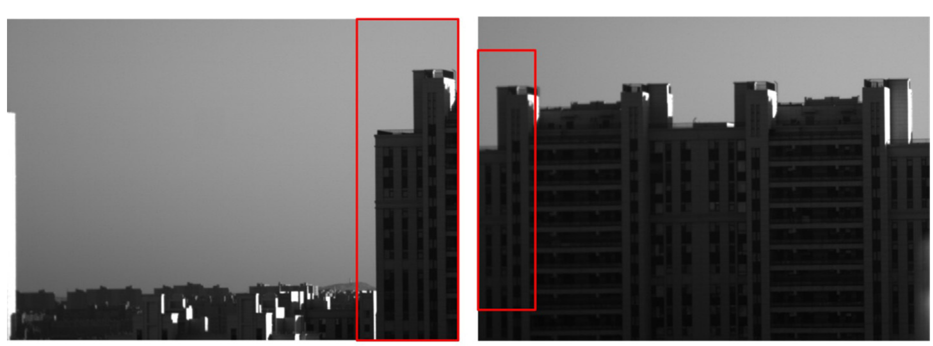

(a) (b)

Fig. 11 Two adjacent images in Fig. 10.

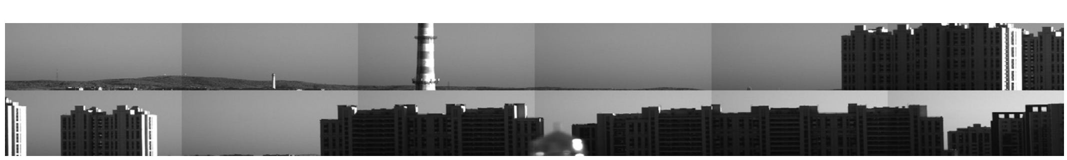

Fig. 12 Twelve unfused images to be registered that were stitched using our proposed algorithm.

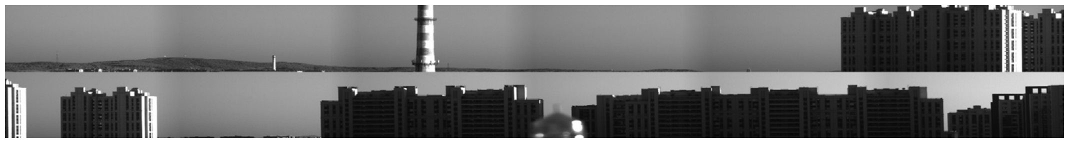

Fig.13 Twelve fused registration images originally stitched using our proposed algorithm.

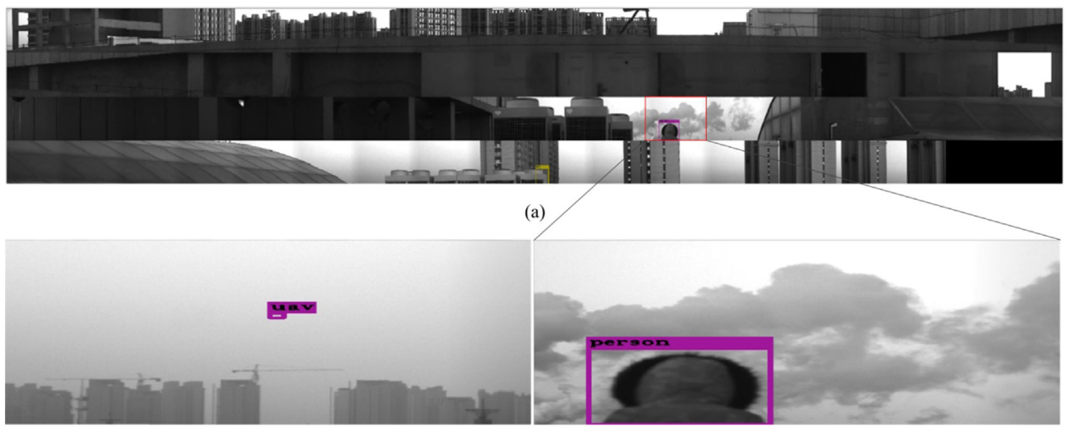

(a)

(b) (c)

Fig. 14 Panoramic target recognition from fused registered images.

results, leading to considerable increases in both false and missed detection rates.

Fig. 11 shows the two adjacent images in Fig. 10; it can be seen that the right side of Fig. 11(a) and the left side of Fig. 11 (b) have overlapping areas, when the image is registered, The inner part of the red box in (a) is used as the source image. The inner part of the red box in (b) is used as a template image. The template image is a subgraph of the source image. The offset in these images is obtained using the proposed registration method.

Fig. 12 shows the stitched image obtained using our proposed registration algorithm. As can be seen from the figure, after registration, the image is aligned in both the vertical and horizontal directions, but gaps can be clearly seen between each pair of images; this is because of a phenomenon similar to vignetting caused by a non-ideal lens. This result indicates that our algorithm is robust to vignetting in practice.

However, in order to get a more natural panorama, we use linear fusion to eliminate the stitching gap in Fig. 12; the resulting image is shown in Fig. 13.

The registered and stitched images were then used for target recognition and detection. This task was achieved using yolo, which is a deep learning-based target detection algorithm. Fig. 14 shows the result of image stitching and target detection for the panoramic target detection system. The panoramic image in Fig. 14(a) consists of 4 rows and 18 columns with a total of 72 images stitched together. Fig. 14(b) shows a detected drone, while Fig. 14(c) shows a detected person. The target type and location can be used for early warning security systems. Thus, our experiments show that using image registration and image fusion to improve image quality can improve the overall accuracy of target detection.

5. Conclusions

In this work, we presented a pyramid PCA for image registration. Our proposed algorithm was shown to be strongly robust to cases wherein the target is partially lost or occluded; in addition, it enabled faster registration compared with traditional registration algorithms. Our proposed method is based on the idea of pyramid decomposition between the source and template images; in particular, phase correlation calculations are performed from the highest level to lowest level in the pyramid to obtain the final registration position. We compared the proposed algorithm with those proposed in and , and found that the peak position of the inverse Fourier transform in the phase correlation spectrum is always constant when the positioning target portion is missing. Nevertheless, in the case of significant noise in the image, the performance of our algorithm will degrade. Thus, as future work, we aim to improve the robustness of the proposed algorithm to image noise.

Declaration of Competing Interest

The authors declare that they have no known competing financial interests or personal relationships that could have appeared to influence the work reported in this paper.

References

[1] B. Zitova, J. Flusser, Image registration methods: A survey, Image Vision Computing 21 (11) (2003) 977–1000.
[2] G. Bartoli, Image registration techniques: A comprehensive survey, Visual Information Processing and Protection Group (2007) 1–54.

[3] N.P. Singh, V.P. Singh, Efficient segmentation and registration of retinal image using gumble probability distribution and brisk feature, Traitement du Signal 37 (5) (2020) 855–864.

[4] M. Deshmukh, U. Bhosle, A survey of image registration. International Journal of Image Processing (IJIP) 5 (3) (2011) 245.

[5] Y. Zhang, S. Qiao, L. Sun, Q. Shi, W. Huang, L. Li, Z. Yang, Photoinduced active terahertz metamaterials with nanostructured vanadium dioxide film deposited by sol-gel method, Optics Express 22 (9) (2014) 11070–11078.

[6] Y. Dong, T. Long, W. Jiao, G. He, Z. Zhang, A novel image registration method based on phase correlation using low-rank matrix factorization with mixture of gaussian, IEEE Transactions on Geoence & Remote Sensing 56 (2017) 446–460.

[7] C.W. Wang, S.M. Ka, A. Chen, Robust image registration of biological microscopic images, Scientific Reports 4 (2014) 6050.

[8] C. Lee, H. Wang, J. Lai, Y. Chang, C. Huang, Automatic marker-free longitudinal infrared image registration by shape context based matching and competitive winner-guided optimal corresponding, Scientific Reports 7 (2017) 39834.

[9] J.M. Guyader, W. Huizinga, D.H. Poot, M. van Kranenburg, A. Uitterdijk, W.J. Niessen, S. Klein, Groupwise image registration based on a total correlation dissimilarity measure for quantitative MRI and dynamic imaging data, Scientific Reports 8 (2018) 13112.

[10] S. Leprince, S. Barbot, F. Ayoub, J.P. Avouac, Automatic and precise orthorectification, coregistration, and subpixel correlation of satellite images, application to ground deformation measurements, IEEE Transactions on Geoscience and Remote Sensing 45 (2007) 1529–1558.

[11] P. Ge, C. Lan, H. Wang, An improvement of image registration based on phase correlation, Optik - International Journal for Light and Electron Optics 125 (2014) 6709–6712.

[12] H.Y. Shum, R. Szeliski, Systems and experiment paper: construction of panoramic image mosaics with global and local alignment, International Journal of Computer Vision 36 (2000) 101–130.

[13] R. Szeliski, Image mosaicing for tele-reality applications, in: Proceedings of 1994 IEEE Workshop on Applications of Computer Vision, 1994, pp. 44–53.

[14] I. Zoghlami, O. Faugeras, R. Deriche, Using geometric corners to build a 2d mosaic from a set of images, Proceedings of IEEE Computer Society Conference on Computer Vision and Pattern Recognition (1997) 420–425.

[15] R. Hartley, A. Zisserman, Multiple view geometry in computer vision, Cambridge University Press, 2000.

[16] D. Capel, A. Zisserman, Automated mosaicing with super-resolution zoom, Proceedings of IEEE Computer Society Conference on Computer Vision and Pattern Recognition (1998) 885–891.

[17] C.D. Kuglin, D.C. Hines, The phase correlation image alignment method, in: Proceedings of IEEE 1975 International Conference on Cybernetics and Society, 1975, pp. 163–165.

[18] J.L. Horner, P.D. Gianino, Phase-only matched filtering, Applied optics 23 (1984) 812–816.

[19] S. Alliney, C. Morandi, Digital image registration using projections. IEEE Transactions on Pattern Analysis, Machine Intelligence (1986) 222–233.

[20] E. De Castro, C. Morandi, Registration of translated and rotated images using finite Fourier transforms, IEEE Transactions on Pattern Analysis Machine Intelligence (1987) 700–703.

[21] D.J. Lee, T.F. Krile, S. Mitra, Digital registration techniques for sequential fundus images, Technical Symposium. International Society for Optics and Photonics (1988) 293–300.

[22] Y. Sheng, H.H. Arsenault, Experiments on pattern recognition using invariant Fourier-mellin descriptors, Journal of the Optical Society of America A Optics & Image Science 3 (1986) 771–776.

[23] R. Rajendran, S.P. Rao, K. Panetta, S.S. Agaian, Adaptive alpha-trimmed correlation based underwater image stitching, in: 2017 IEEE International Symposium on Technologies for Homeland Security (HST), 2017, pp. 1–7.

[24] E. Adel, M. Elmogy, H. Elbakry, Image stitching based on feature extraction techniques: a survey, International Journal of Computer Applications 99 (2014) 1–8.

[25] E. de Castro, C. Morandi, Registration of translated and rotated images using finite Fourier transforms, IEEE Transactions on pattern analysis and machine intelligence 5 (1987) 700–703.

[26] V. Leclerc, C. Benchimol, Automatic elastic registration of DSA images, Computer assisted radiology (1987) 719–723.

[27] Q. Chen, Image registration and its applications in medical imaging PhD thesis, Vrije University, Brussels, Belgium, 1993.

[28] H. Shekarforoush, M. Berthod, J. Zerubia, Subpixel image registration by estimating the polyphase decomposition of cross power spectrum, Proceedings of IEEE Computer Society Conference on Computer Vision and Pattern Recognition (1996) 532–537.

[29] J. Wang, L.E. Reinstein, J. Hanley, A.G. Meek, Investigation of a phase-only correlation technique for anatomical alignment of portal images in radiation therapy, Physics in medicine and biology 41 (1996) 1045–1058.

[30] M. Xu, P.K. Varshney, A subspace method for fourier-based image registration, geoscience and remote sensing letters, IEEE Geoscience and Remote Sensing Letters 6 (3) (2009) 491–494.

[31] G.Q. Maguire, M.E. Noz, E.M. Lee, J.H. Schimpf, Correlation methods for tomographic images using twoand three-dimensional techniques, Information Processing in Medical Imaging (1986) 266–279.

[32] P.R. Krishnaveni, G.N. Kishore, Image based group classifier for brain tumor detection using machine learning technique, Traitement du Signal 37 (5) (2020) 865–871.

[33] A. Collignon, Multi-modality medical image registration by maximization of mutual information Ph.D. Thesis, Catholic University of Leuven, Leuven, Belgium, 1998.

[34] A. Bala, A. Rani, S. Kumar, An illumination insensitive normalization approach to face recognition using locality sensitive discriminant analysis, Traitement du Signal 37 (3) (2020) 451–460.

[35] S. Sanjay-Gopal, H.P. Chan, T. Wilson, M. Helvie, N. Petrick, B. Sahiner, A regional registration technique for automated interval change analysis of breast lesions on mammograms, Medical Physics 26 (12) (1999) 2669–2679.

[36] O. Samritjiarapon, O. Chitsobhuk, An FFT-Based Technique and Best-first Search for Image Registration, International Symposium on Communications and Information Technologies (2008) 364–367.

[37] R. Reed, Comparison of subpixel phase correlation methods for image registration, Arnold Engineering Development Center Arnold Air Force Base, Tenn, 2010.

[38] F. Alsaade, Fast and accurate template matching algorithm based on image pyramid and sum of absolute difference similarity measure, Research Journal of Information Technology 4 (4) (2012) 204–211.

[39] E.H. Adelson, C.H. Anderson, J.R. Bergen, P.J. Burt, J.M. Ogden, Pyramid methods in image processing, RCA engineer 29 (1984) 33–41.

[40] P. Burt, E. Adelson, The laplacian pyramid as a compact image code, IEEE Transactions on communications 31 (1983) 532–540.

[41] Y. Fouda, K. Ragab, An efficient implementation of normalized cross-correlation image matching based on pyramid, International Joint Conference on Awareness Science and Technology & Ubi-Media Computing (2013) 98–103.